A new approach to hardening mechanisms in the diffusion layer of gas nitrided α-alloyed steels. Effects of chromium and aluminium: experimental and simulation studies

C. Ginter, L. Torchane, J. Dulcy, M. Gantois, A. Malchère, C. Esnouf, T. Turpin

Hardening mechanisms in the diffusion layer of gas nitrided α-iron and -steels have been investigated through the study about effects of chromium (binary alloys and industrial steels) and aluminium (industrial steel). After nitriding (520°C 48h), nitrogen mass balance between total nitrogen concentration located in the diffusion zone, experimentally determined, and the expected theoretical nitrogen concentration, reveals for each alloy a "nitrogen excess". Jack and Mittemeijer [1-3] suggested that the volume misfit between semi-coherent nitrides and matrix induces local matrix lattice distorsion, leading to a local increase of nitrogen solubility in the matrix.

We propose a new approach, based on thermodynamical calculations (Thermo-Calc software), confirmed by different characterization methods (HRTEM, EDX and X-Ray). Indeed no significant solid solution "N excess" occurs, but the total nitrogen concentration is explained by complex MN nitrides precipitation, isomorph of CrN FCC, containing chromium, iron (up to 30at.% at 50µm from the surface), molybdenum and vanadium. During annealing (520°C 48h), atomic iron fraction in MN nitrides decreases and the corresponding nitrogen atomic fraction diffuses to the core.

Addition of aluminium in industrial steel strongly increases nitrogen concentration and hardening ($\Delta = HV_x - HV_{initial}$). Aluminium induces in the diffusion layer precipitation of Fe_4N and $Fe_{2-3}N$ and precipitates in complex MN FCC nitrides, containing chromium, iron and molybdenum.

INTRODUCTION

Gas-nitriding is a thermochemical treatment, applied in aeronautic and automotive industries, to improve the fatigue resistance, tribological and anticorrosion properties. The nitrided case can be divided, as a general rule, into a compound layer adjacent to the surface (thickness about $10\mu m$) and a diffusion zone (depth up to 1µm). This study concerns only the diffusion zone. Relationship between nitrogen concentration and hardness are strongly dependant of steel composition and microstructure: different hardening mechanisms occur, depending of nitriding time and temperature.

The purpose of this paper is to propose a new explanation about nitrogen localization and improve hardening mechanisms understanding. Thus effects of chromium and aluminium were investigated through experimental, simulation and characterization studies.

Caroline Ginter
Laboratoire de Sciences et Génie des Surfaces (LSGS), Ecole des Mines, Nancy, France
Aubert et Duval, Eramet Group

L. Torchane, J. Dulcy, M. Gantois
Laboratoire de Sciences et Génie des Surfaces (LSGS), Ecole des Mines, Nancy, France

Annie Malchère, C. Esnouf
Laboratory GEMPPM, CECM Group, INSA Lyon, France

T. Turpin
Aubert et Duval, Eramet Group

Binary and ternary alloys have been the subject of many investigations [1,2,4,5,6], which showed that aluminium and chromium increase nitrogen content and hardness, due to the chromium nitrides FCC semi-coherent precipitation. Nevertheless mechanisms due to aluminium are not clear [7-9]. Moreover hardening mechanisms in industrial steels are complex and at this time not really understood, in spite of two important studies about 32CrMoV13 steel [10,11], which suggested interesting mechanisms related to the chromium presence.

Therefore it was first necessary to determine nitrogen localization on binary alloys, and explain the "N excess" observed by numerous authors in binary and ternary alloys [1,2,12,13,14]. Then, using the same methodology (experiment, simulation, characterization) on industrial alloys, nitrogen localization identification in industrials steels allowed to suggest several hardening mechanisms, related to chromium and aluminium presence.

MATERIALS AND EXPERIMENTAL PROCEDURE

Materials investigated in this work are binary alloys (1, 3 and 5wt.%Cr) and about 14 industrial α-alloyed steels manufactured by Aubert et Duval (heated, quenched then annealed). Two industrial steels were specially studied; their chemical composition is given in Table 1.
Samples were gas-nitrided in a vertical furnace during 48h at 520°C, then quenched in water. The thermogravimetric measurements were useful to follow the nitrogen mass tran-

Steel	wt.%C	wt.%Si	wt.%Mn	wt.%Ni	wt.%Cr	wt.%Mo	wt.%V	wt.%Al	HV50 Initial
K	0.318	0.287	0.532	0.09	3	0.83	0.27	0.013	329
I	0.311	0.330	0.560	0.13	1.73	0.30		0.94	296

Table 1 – Chemical composition and initial hardness of K and I industrial steels.

Tabella 1 – Composizione chimica e durezza iniziale degli acciai industriali K e I.

sfer through the material from the gas/solid interface. Some of them were then annealed, in N_2 atmosphere, during 48h at 520°C, then quenched in water.

Nitrided and annealed samples were mechanically characterized with a micro-hardness tester. Nitrogen profiles in the nitrided zone were determined from the sample surface through an electron microprobe analysis. Phases identification was carried out using X-Ray θ-2θ diffractometer, employing CoKα radiation.

Nitrides and carbides were examined through Transmission Electron Microscopy, using a Jeol 200CX (200kV) for conventional imaging and a Jeol 2010F with a field emission gun for high resolution imaging and nanoanalysis, equipped with an INCA Energy Dispersive X-Ray System from Oxford, with polymer ultra-thin window. TEM observations were performed on extraction replicas and thin foils. Extraction carbon replicas were collected on copper grid, after carbon film deposition on a polished surface and nital ($1.4\%HNO_3$ + ethanol) chemical etching. Thin foils were prepared by spark eroding discs of 3mm diameter (initially about 700µm in depth), then mechanically polished with a tripod polisher up reaching 20 to 50µm in depth, to be finally ion thinned.

Thermodynamical calculations were performed with Thermo-Calc software, based on Gibb's free energy minimization of the defined system. Phases (molar fraction with atomic chemical composition) appearing at the chemical equilibrium were simulated, from experimental data (nitriding temperature, alloy chemical composition, nitrogen concentration).

I - Binary alloys - Chromium effect

It is well known that nitrogen concentration and hardness profiles after nitriding depend on chromium concentration. Indeed, due to the strong Cr-N affinity, chromium combines with nitrogen to precipitate as fine semi-coherent nitride CrN FCC, directly responsible for observed hardening.

As hardening mechanisms in industrial steels revealed really complex, a preliminary work was conducted on binary alloys. It should be noticed that a discontinuous precipitation, already observed by several authors [3,11,15,16,17,18,19], occurs in Fe-3wt.%Cr (Fig.1) and 5wt.%Cr alloys, leading to a hardness decrease (about 200HV) and does not occur in steels. Consequently, the objective of this work on binary alloys was concentrated on nitrogen localization and role. The Fe_4N phase often grows at grain boundaries at the compound and diffusion layers interface, up to 10 or 20µm at the beginning of the diffusion layer. Consequently, it was decided to investigate the diffusion layer from 50µm below the surface. Three binary alloys (1, 3 and 5wt.%Cr) were nitrided at 520°C during 48h with $Kn = P(NH_3)/P(H_2)^{3/2}$ of 1, then mass nitrogen concentration profiles were performed (Fig. 1). Nitrogen mass balance was determined for each alloy as follows: N theoretical, called from now LCth (mass nitrogen Limited Concentration), subtracted from total amount of N absorbed [N_{total}], experimentally determined, revealed N excess for each alloy below the surface. LCth is defined as the nitrogen mass concentration involved in nitride precipitation CrN [N_{CrN}] and the nitrogen mass concentration dissolved in the matrix [N_α] (0.043wt.%N at 520°C [20]). LCth depends on nitriding temperature and alloy chemical composition

Chromium Effect on Nitrogen Concentration

5wt.%Cr — 1.83wt.%N 14.5mol.%$(Cr_{0.70},Fe_{0.30})$N
LCth 1.35wt.%N 11mol.%CrN
3wt.%Cr — 1.12wt.%N 9mol.%$(Cr_{0.78},Fe_{0.22})$N
LCth 0.8wt.%N 6mol.%CrN
1wt.%Cr — 0.42wt.%N 3mol.%$(Cr_{0.72},Fe_{0.28})$N
LCth 0.27wt.%N 2mol.%CrN
Nitriding 520°C Kn1 48h

Legend: Fe - 1wt.% Cr · Fe - 3wt.% Cr · Fe - 5wt.% Cr

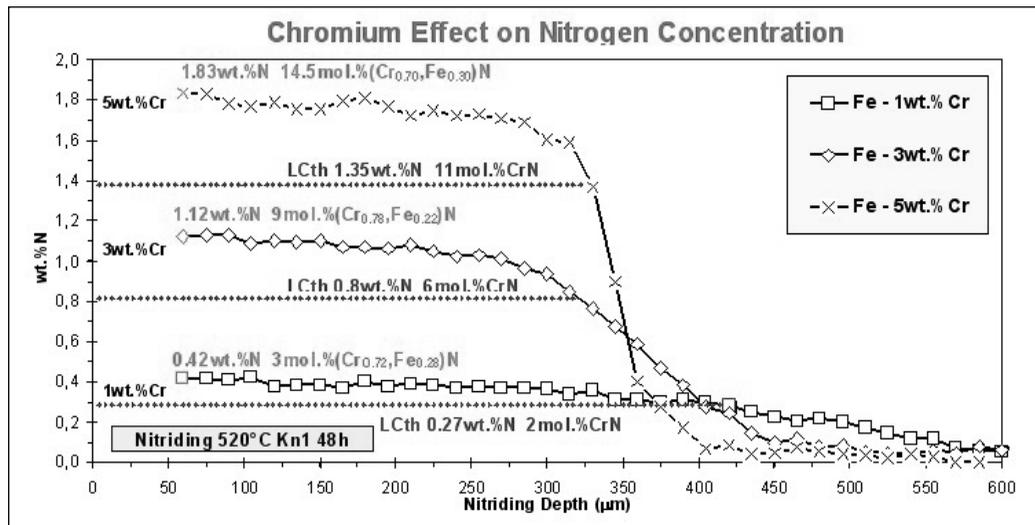y-axis: wt.%N — x-axis: Nitriding Depth (µm)

Fig. 1 – Mass Nitrogen concentration profiles versus nitriding depth of Fe - 1, 3 and 5wt.%Cr alloys, nitrided at 520°C during 48h with Kn 1. Thermo-Calc phases simulation at 50µm from the surface and at LCth, for each alloy.

Fig. 1- Profili della concentrazione totale di azoto in rapporto alla profondità di nitrurazione delle leghe Fe - 1, 3 e 5wt.% Cr, nitrurate a 520°C per 48h con Kn 1. Simulazione delle fasi mediante Thermo-Calc a 50µm dalla superficie ed alla LCth(mass nitrogen Limited Concentration), per ogni lega.

Binary Alloys / T6 520°C Kn1 48h	wt.%N LCth	wt.%Nexp 50µm surface	wt.%N Excess 50µm surface
Fe - 1wt.%Cr	0.27	0.44	0.13
Fe - 3wt.%Cr	0.80	1.13	0.29
Fe - 5wt.%Cr	1.35	1.84	0.45

Table 2 – Three binary alloys nitrided at 520°C during 48h with a Kn of 1. Determination of nitrogen excess at 50µm from the surface, from LCth (wt.%N) and experimental mass nitrogen concentration determined at 50µm from the surface values.

Tabella 2 – Tre leghe binarie nitrurate a 520°C durante 48h con un Kn di 1. Determinazione dell'eccesso di azoto: a 50µm dalla superficie, dalla LCth (mass nitrogen Limited Concentration - N peso %), concentrazione totale di azoto determinata sperimentalmente a 50µm dai valori di superficie.

Fig. 2 – Mass Nitrogen concentration profiles versus nitriding depth of Fe - 3wt.%Cr alloy, nitrided at 520°C during 48h with Kn 1, then annealed at 520°C during 48h (from electron microprobe analysis). Thermo-Calc phases simulation at 50µm from the surface after nitriding and at LCth. Micrograph of the nitrided zone showing discontinuous precipitation below the surface.

Fig. 2 – Profili della concentrazione totale di azoto (dall' analisi con microsonda elettronica) in rapporto alla profondità di nitrurazione nella lega Fe - 3 % in peso Cr, nitrurata a 520°C per 48h con Kn 1, quindi sottoposta a trattamento a 520°C per 48h. Simulazione delle fasi mediante Thermo-Calc a 50µm dalla superficie ed alla LCth. Micrografia della zona nitrurata che mostra la precipitazione discontinua sotto la superficie.
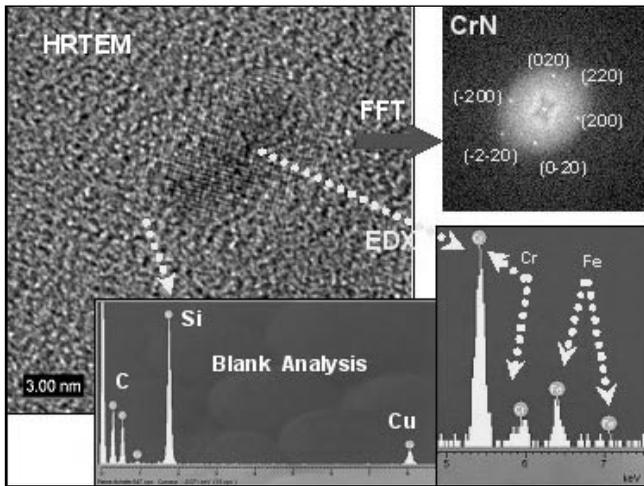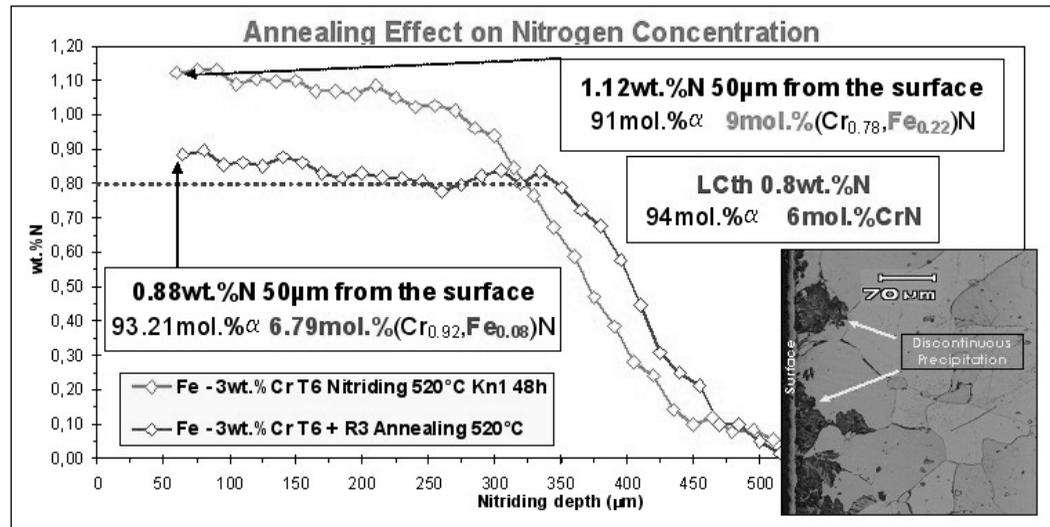

Fig. 3 (left) – Fe-3wt.%Cr, nitrided at 520°C during 48h, nitrides extracted on carbon replicas at 50µm from the surface, investigated with HRTEM and EDX. HRTEM precipitate image and corresponding Fourier Transformation (calculated diffraction pattern obtained) confirmed that the precipitate is CrN FCC. The EDX analysis revealed the presence of iron in the nitride. Blank analysis, close to the precipitate, allowed to identify peaks due to the environment (copper from the grid, carbon and silicon from the carbon deposition), and ensure that no matrix was extracted.

Fig. 3 (sinistra) – Lega Fe-3 % in peso Cr, nitrurata a 520°C per 48h; nitruri estratti con repliche di carbonio a 50µm dalla superficie, esaminata con HRTEM e EDX. L'immagine HRTEM del precipitato e la corrispondente trasformata di Fourier (ottenuta l'immagine di diffrazione calcolata) hanno confermato che si tratta del precipitato CrN FCC. L'analisi EDX ha rivelato la presenza di ferro nel nitruro. L'analisi di confronto, vicino al precipitato, ha permesso di identificare picchi dovuti all'ambiente (rame dalla griglia, carbonio e silicio dal deposito di carbonio) e assicura che non è stata estratta anche parte della matrice.

(see Table 2). Fig. 1 and Table 2 show that nitrogen concentration raises with increase of chromium concentration, associated with a molar fraction nitrides precipitation predicted by Thermo-Calc, linked to a hardness increase, as reported by Hekker [2]. These results show that nitrides are directly responsible for hardness.

Nitrogen concentration enhances with chromium concentration increase (as shown in Table 2). According to Thermo-Calc calculations at 50μm from the surface (Fig.1), no significant solid solution nitrogen excess occurs, but nitrogen content from LCth depth up to the surface is explained by the iron precipitation in complex MN nitrides, isomorph of CrN FCC (about 30at.%). Indeed the iron presence leads to increase nitrogen concentration involved in nitrides MN precipitation and enables nitrogen mass balance to be equilibrated. Note that the iron atomic radius (0.1241nm) is similar to the chromium radius (0.1249nm) and FeN, obtained by PVD (lattice parameter 0.430nm), is isomorph of CrN FCC (lattice parameter 0.414nm). Iron acts like chromium, allowing nitrides to keep the same size, morphology, semi-coherence with the matrix and so possibly the same effect on hardness.

In order to check nitrogen mobility, nitrided Fe-3wt.%Cr alloy was annealed at nitriding temperature and time (520°C, 48h). Fig. 2 shows nitrogen profiles after nitriding and after annealing versus nitriding depth, and confirms that nitrogen diffuses to the core. After annealing, nitrogen concentration profile presents a plateau, coinciding with LCth. Thermo-Calc results (fraction phases with chemical composition, at 50μm from the surface for both of them and at LCth depth) are also plotted on Fig. 2. Thermo-Calc indicates that during annealing, the phase $(Fe_x,Cr_y)N$ tends to a more stable phase CrN, leading to loss of iron - about 22at.% - (and corresponding nitrogen atomic fraction) associated with the molar fraction nitrides decrease by about 33% (9mol.% to 6.8mol.%), which also should contribute to decrease the hardness, too.

Microstructural characterizations were performed on nitrides from carbon replicas and thin foils with High Resolution Transmission Electron Microscopy and Energy Dispersive X-Ray. For both cases after nitriding and after annealing, at 50μm from the surface, precipitates with platelet morphology, present at grain boundaries and in discontinuous precipitation, were confirmed by High Resolution Image Fourier Transformation to be chromium nitrides CrN FCC. Then EDX analysis was performed on them, after verification close to the precipitate that the ferritic matrix was not extracted.

In the first case, after nitriding, EDX analysis (Fig.3) confirmed that nitrides (10 to 20nm diameter, 2-10nm thick) contain iron, with an iron fraction distribution of 14-37at%, in agreement with Thermo-Calc prediction (22at.%Fe).

In the second case, after annealing, Thermo-Calc predicts an iron concentration of 8at.% in nitrides. Actually, the coarser nitrides (20nm diameter), after EDX analysis (Fig.4), contain from 5 to 14at.%Fe. These investigations confirmed that nitrides lost iron and corresponding nitrogen (1 to 1 atom) during annealing, the released nitrogen diffusing to the core.
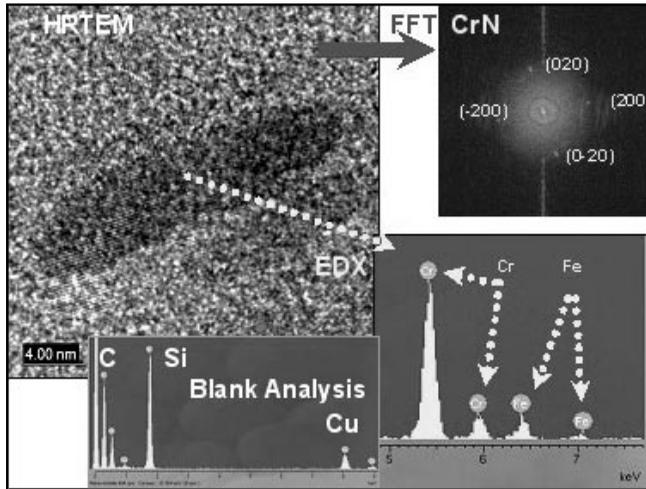
Fig. 4 (right) – Fe-3wt.%Cr, nitrided at 520°C during 48h then annealed at 520°C during 48h, nitrides extracted on carbon replicas at 50µm from the surface, investigated with HRTEM and EDX. HRTEM precipitate image and corresponding Fourier Transformation (calculated diffraction pattern obtained) confirmed that the precipitate is CrN FCC. The EDX analysis revealed the presence of iron in the nitride, but less than in previous case (Fig.3). The EDX analysis revealed the presence of iron in the nitride. Blank analysis, close to the precipitate, allowed to identify peaks due to the environment (copper from the grid, carbon and silicon from the carbon deposition), and ensure that no matrix was extracted.

Fig. 4 (destra) – Lega Fe-3 % in peso Cr, nitrurata a 520°C per 48h quindi sottoposta a trattamento a 520°C per 48h: nitruri estratti con repliche di carbonio a 50µm dalla superficie, esaminati con HRTEM e EDX. L'immagine HRTEM del precipitato e la corrispondente trasformata di Fourier (ottenuta l'immagine di diffrazione calcolata) hanno confermato che il precipitato è CrN FCC. L'analisi EDX ha rivelato la presenza di ferro nel nitruro, ma in quantità minore rispetto al caso di Fig.3. L'analisi di confronto, vicino al precipitato, ha permesso di identificare i picchi dovuti all'ambiente (rame dalla griglia, carbonio e silicone dal deposito di carbonio) e assicura che non è stata estratta anche parte della matrice.

II - Industrial steels

A nitriding treatment (520°C 48h Kn3) on 14 different industrial steels put into evidence the well known preponderant roles of chromium and aluminium on nitrogen concentration and hardness profiles. As in binary alloys, a chromium content increase leads to nitrogen concentration and hardness enhancements, due to a semi-coherent fine MN FCC precipitation fraction augmentation. Two steels were selected to be representative of chromium effect (K 3wt.%Cr) and alu-

minium effect (I 1.73wt.%Cr 0.94wt.%Al).
The same methodology applied to binary alloys was used to study both industrial steels:
• Experiment and first characterization : nitriding then nitrogen concentration and hardness profiles performed,
• Phases (molar fraction and chemical composition) simulations by means of the software Thermo-Calc,
• TEM and EDX characterization on nitrides and carbides.

A - Chromium effect: K steel
K steel, which contains 3wt.%Cr, was nitrided at 520°C during 48h. Nitrogen concentration and hardness profiles were performed then Thermo-Calc calculations at 50µm from the surface. Hardening (HV_x - $HV_{initial}$) is represented as a nitrogen concentration function (Fig.5). Yet Thermo-Calc predicts that nitrides fraction keeps on rising linearly with nitrogen concentration. It can be deduced then that nitrides precipitation contributes directly to hardening. Another interesting result of Thermo-Calc calculations (molar fraction phase versus nitrogen concentration) is that nitride precipitation requires the entire carbides transformation, in order to release chromium, vanadium and molybdenum.
Thermo-Calc does not make the difference between vanadium carbide, vanadium carbonitride and chromium nitride, as they crystallize in the same structure FCC with a similar lattice parameter. As reported by Locquet [10], vanadium carbides, present before nitriding, transform into carbonitride V(C,N), keeping the same size, morphology and localization. Considering that result, they should keep the same molar fraction, which is small (0.58mol.%) compared to the MN+V(C,N) one, predicted by Thermo-Calc at 50µm from the surface (9.52mol.%).
At 50µm from the surface, nitrogen mass concentration raises to 1.27wt.%N. Considering that LCth, calculated including chromium, vanadium and molybdenum, is 1.00wt.%N, a "N excess" was revealed equal to 0.28wt.%N. Nitrogen concentration is once again explained, according to Thermo-Calc calculations, by the iron alloying in MN complex nitrides (M stands for Molybdenum, Vanadium and Chromium), isomorph of CrN FCC. Iron, molybdenum and vanadium seem to act like chromium and keep the same role towards hardening mechanisms (especially MN FCC semi-coherent nitrides).
Some investigations on thin foils at 50µm from the surface after nitriding, which revealed two different MN precipitations, as reported by Locquet [10]. Indeed globular nitrides indexed as MN FCC germinate at the matrix/carbide interface, due to carbides transformation. Diffraction patterns and corresponding dark field revealed the presence of semi-coherent finer nitrides MN FCC, with platelet morphology,
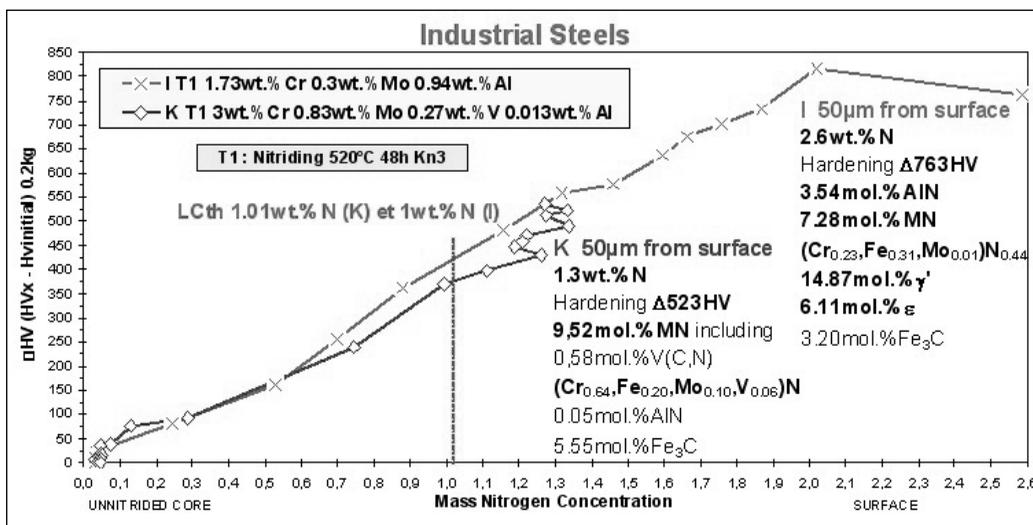

Fig. 5 – Hardening (HVx - HVinitial) representation as a function of mass nitrogen concentration of I and K steels, nitrided at 520°C during 48h with a Kn of 3. Phases (molar fraction and chemical composition) simulation by Thermo-Calc at 50µm from the surface.

Fig. 5 – Rappresentazione dell'indurimento (HVx - HViniziale) in funzione della concentrazione totale di azoto negli acciai K e I, nitrurati a 520°C per 48h con un Kn di 3. Simulazioni di fasi (frazione molare e composizione chimica) mediante Thermo-Calc a 50µm dalla superficie.

due to the nitrogen and elements dissolved in the matrix combination.

Presently, hardening mechanisms could be related as follows (from [10,11] and Thermo-Calc calculations):

• Fine semi-coherent nitrides MN FCC (M stands for Fe, Cr, Mo and V) precipitate from the combination of nitrogen and elements dissolved in the matrix. They are known to contribute in a large part to nitriding hardening.

• $M_{23}C_6$ carbides (inter- and intragranular) transform into globular mixed (Fe, Cr, Mo, V)N FCC nitrides. The chemical composition of these nitrides will be soon investigated. Their contribution to nitriding hardening is not already clearly identified.

• Vanadium carbides present before nitriding transform into carbonitride V(C,N), and can not induce more hardness.

B - Aluminium effect: I steel

Both steels I (1.73wt.%Cr and 0.94wt.%Al) and K (3wt. %Cr) were nitrided at 520°C during 48h with a Kn of 3. Nitrogen concentration and hardness profiles were performed. Then the hardening (HV_x - $HV_{initial}$) has been represented as a function of mass nitrogen concentration, Fig. 5. Even though both steels have the same CLth (the same nitrogen concentration involved in (Cr, Mo, V, Al)N precipitation), steel I shows a nitrogen concentration at 50μm from the surface of 2.6wt.%N (1.3wt.%N for steel K), and hardening (Δ=HV_x-$HV_{initial}$) of 763HV (536HV for steel K)!

Nitrogen concentration below the surface is explained first by thermodynamical simulation and confirmed by HRTEM and EDX, as the iron alloying in complex MN FCC nitrides (M = Cr, Mo, V) for both steels I and K. Nevertheless the iron concentration seems to be limited to about 20at.%. Thermo-Calc predicts hexagonal AlN precipitation, but they were not observed. In industrial steels, iron and aluminium combine with chromium and molybdenum to form (Cr, Mo, Fe, Al)N FCC precipitates (chemical composition is given Table 3).

Nitrogen concentration observed in I steel is also explained below the surface by the γ' (Fe_4N) and ε ($Fe_{2-3}N$) precipitation in the diffusion layer, confirmed by X-Ray analysis, up to 125μm in depth in the diffusion layer, which corresponds to 1.8wt.%N.

Presently, hardening mechanisms could be explained as follows:

• Semi-coherent platelets were analyzed and identified as complex MN (M = Fe, Al, Cr, Mo) FCC. Iron would be contained in MN from LCth depth up to the surface. These nitrides, known to contribute mainly to hardening (ΔHV), are the result of the combination of nitrogen and elements dissolved in the matrix. Thermo-Calc simulation of the matrix composition before nitriding for steels I and K (Table 4) shows that the nitrogen concentration involved in MN semi-coherent precipitation is twice more important for I steel than for K steel, which could explain the huge hardening observed below the surface in I steel.

• $M_{23}C_6$ and M_7C_3 carbides, present in bainitic structure before nitriding, transform into globular incoherent com-
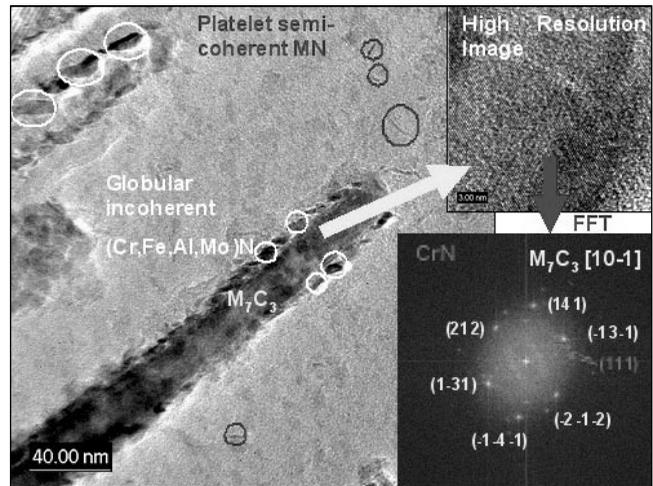

Fig. 6 (left) – I steel (1.73wt.Cr 0.94wt.%Al), nitrided at 520°C during 48h. Nitrides were extracted on carbon replicas at 50μm from the surface, investigated with HRTEM and EDX. HRTEM precipitate image and corresponding Fourier Transformation (calculated diffraction pattern obtained) confirmed that elongated carbide M7C3 transform partially into globular nitrides (Cr, Fe, Al, Mo)N FCC.

Fig. 6 (sinistra) – Acciaio I (1.73% Cr e 0.94wt.% Al), nitrurato a 520°C per 48h. Sono stati estratti nitruri su repliche di carbonio a 50μm dalla superficie, esaminati mediante HRTEM e EDX. L'immagine del precipitato HRTEM e la corrispondente trasformata di Fourier (ottenuta l'immagine di diffrazione calcolata) hanno confermato che il carburo allungato M7C3 si trasforma parzialmente in nitruri globulari (Cr, Fe, Al, Mo)N FCC.

plex MN FCC (M stands for Cr, Al, Mo and Fe - Fe below the surface up to LCth depth -). Elongated carbides transform only partially into nitrides (as observed Fig.6), but globular ones, which are smaller, transform wholly (as observed Fig.7). These nitrides germinate at the matrix/carbide interface. Their contribution to nitriding hardening is not yet clearly identified.

• If γ' and ε precipitate with well-known needle morphology in lath interfaces, it can be expected that their contribution to hardening is not significant.

CONCLUSION

Thermo-Calc calculation associated with microstructural analysis (HRTEM and EDX) allows the determination of nitrogen localization, which leads to a better understanding of chromium and aluminium effects on hardening mechanisms.

Binary Alloys

1- Chromium concentration increase in binary alloys induces nitrogen content enhancement, linked to MN FCC nitrides fraction and hardness augmentation, showing that semi-coherent MN nitrides are responsible for hardening.

Table 3 – I steel nitriding at 520°C during 48h. Results of EDX analysis (average and range) performed on nitrides extracted at 50μm from the surface, with corresponding sizes.

Tabella 3 – Nitrurazione dell'acciaio I a 520°C per 48h. Risultati dell'analisi EDX (media e intervallo dei valori) effettuata sui nitruri estratti a 50μm dalla superficie, con le corrispondenti dimensioni.

ITI 50µm surface MN FCC		M Chemical composition (at.%)				Size (nm)
		Al	Cr	Fe	Mo	
Semi-coherent platelets	Average / 3 zones	45	18	23	13	3-13
	Range	41-49	13-24	19-29	6-17	length
Globular germinated at the carbides/α interface	Average / 22 particles	13	73,5	7	7	6-28
	Range	3-23	61-82	2-13	1-12	length
Bainitic lath interface	Average / 4 zones	61	18	8	13	3-9
	Range	57-66	12-26	4-12	9-16	length

Phases molar fraction / Chemical mass composition α	wt.%Cr$_\alpha$	wt.%Mo$_\alpha$	wt.%V$_\alpha$	wt.%Al$_\alpha$	wt.%N$_{MN}$ from α
K core 650°C 5.54mol.%M$_{23}$C$_6$ 0.08mol.%M7C3, 93.77mol.%α	1.16	0.12	0.02	0.01	0.34
I core 620°C 2.61mol.%M$_{23}$C$_6$, 2.86mol.%M$_7$C$_3$, 94.53mol.%α	0.28	0.03		0.98	0.59

Table 4 – From Thermo-Calc simulation of the ferritic phase chemical composition, determination of the mass nitrogen concentration, which could precipitate as semi-coherent MN FCC nitrides with elements dissolved in the matrix - K and I steels - Simulation at the last pre-treatment before nitriding (650°C for K and 620°C for I).

Tabella 4 – Da simulazione Thermo-Calc della composizione chimica della fase ferritica, determinazione della concentrazione totale di azoto, che può precipitare in forma di nitruri semi-coerenti di MN FCC, con M costituito dagli elementi dissolti nella matrice (acciai I e K). Simulazione all'ultimo pretrattamento prima della nitrurazione (650°C per K e 620°C per I).
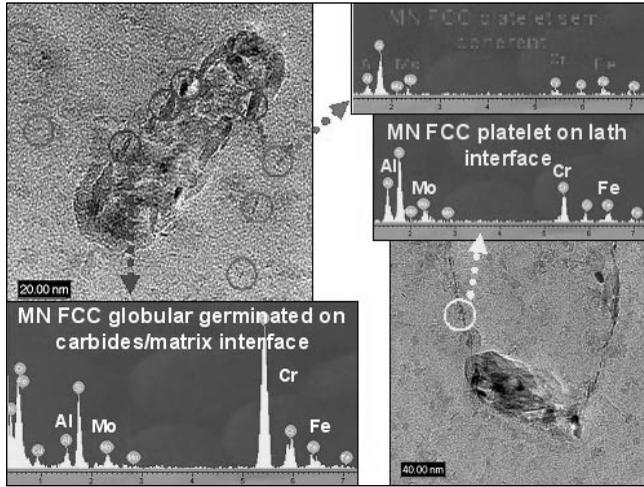

Fig. 7 (right) – HRTEM precipitate image (and Fourier Transform not shown here) and EDX analysis confirmed that globular carbides transform wholly into globular nitrides MN FCC, that semi-coherent platelets are MN FCC and that precipitates on lath interfaces are also MN FCC. M stands for iron, aluminium (in chromium presence, aluminium does not precipitate as hexagonal AlN), chromium and molybdenum.

Fig. 7 (destra) – Immagine HRTEM del precipitato (la trasformata di Fourier non è qui riportata) e analisi EDX hanno confermato che i carburi globulari si trasformano interamente in nitruri globulari MN FCC, che le piastrine semi-coerenti sono MN FCC e che anche i precipitati sulle interfacce sono MN FCC. M sta per ferro, alluminio (in presenza di cromo, l'alluminio non precipita come AlN esagonale), cromo e molibdeno.

2- After nitriding, complex MN (M = Fe and Cr), isomorph of CrN FCC, are observed with a maximum of iron atomic fraction below the surface, which explains nitrogen content. Iron acts like chromium, inducing nitrides fraction and hardening increase. It was confirmed that in the nitrided Fe-3wt.%Cr alloy, at $50\mu m$ from the surface, nitrides MN FCC, with platelet morphology contain between 14 and 37at.%Fe (22at.%Fe simulated by Thermo-Calc).

3- After annealing, under temperature effect nitrogen diffuses to the core. From the surface up to LCth depth, nitrides MN loose partially iron and nitrogen corresponding (1 N atom to 1 Fe atom), decreasing MN molar fraction. From LCth depth up to the core, as all chromium was not used to precipitate, the released nitrogen can combine with chromium, to form CrN and so increase CrN molar fraction and hardening.

Industrial steels

1- After nitriding several industrial a-alloyed steels, it could have been concluded that chromium and aluminium enhance nitrogen concentration and hardness profiles, molybdenum and vanadium having a minor importance.

2- In industrial steels without aluminium, nitrogen mass balance can be explained, according to Thermo-Calc simulations, by complex MN nitrides, isomorph of CrN FCC, containing chromium, iron, molybdenum and vanadium. Before nitriding, the largest part of chromium, molybdenum and vanadium precipitated as carbides VC and $M_{23}C_6$. These last ones transform during nitriding into globular incoherent MN FCC. A small fraction of chromium, molybdenum and vanadium, dissolved in the matrix, combines with nitrogen and precipitates as semi-coherent platelets MN FCC. More HRTEM and EDX investigations will be performed to identify chemical compositions of both kinds of precipitates.

3- In industrial steels, aluminium allows a huge nitrogen concentration and induces significantly important hardening. Below the surface, nitrogen mass balance is first explained, according to Thermo-Calc simulation and confirmed by characterization, by complex nitrides MN, isomorph of CrN FCC, containing iron (atomic fraction seems to be limited to 30at.%), aluminium, chromium and molybdenum. γ' and ε phases precipitation in the diffusion layer allows nitrogen balance to be equilibrated. Another new important result is that aluminium precipitates in complex MN nitrides FCC, and not as hexagonal AlN and contributes to an important hardness increase.

REFERENCES

[1] D.H. JACK, K.H. JACK, Materials Science and Engineering 11, (1973) p. 1-27

[2] P.M. HEKKER, E.J. MITTEMEIJER, H.C.F. ROZENDAAL, The influence of Nitriding on the Microstructure and Stress State of Iron and Steel (1985) p. 51-61

[3] E.J. MITTEMEIJER, H.C.F. ROZENDAAL, P.J. VAN DER SCHAAF, R.T. FURNEE, The influence of Nitriding on the Microstructure and Stress State of Iron and Steel (1985) p. 109-117

[4] B.J. LIGHTFOOT, D.H. JACK, Heat Treatment'73, London, (1973) p. 59-65

[5] H.J. SPIES, S. BÖHMER, HTM 39 (1984) p. 1-6

[6] Y.M. LAKHTIN, Y.D. KOGAN, Mashinostroenie, Moscow, (1976)

[7] V.A. PHILLIPS, A.U. SEYBOLT, Trans. Of the Metall. Society of AIME 242, (1968) p. 2415-2422

[8] H.C.F. ROZENDAAL, E.J. MITTEMEIJER, P.F. COLIJN, P.J. VAN DER SCHAAF, Metall. Trans. A 14, 2 (1983) p. 395-399

[9] J.P. CALVEL, Détermination expérimentale des contraintes résiduelles introduites par la nitruration gazeuse d'aciers 35CD4 et 40CAD6.12 - Relations avec le

durcissement, PhD Thesis INPT, France (1983)

[10] J.N. LOCQUET, R. SOTO, L. BARRALLIER, A. CHARAÏ, Microsc. Microanal. Microstruct. 8 (1997) p. 335-352

[11] M. SENNOUR, Apport de la microscopie électronique en transmission et de la spectroscopie EELS à la caractérisation de nitrures (AlN, CrN) dans le fer et l'alliage Fe-Cr, PhD Thesis INSA Lyon, France (2002)

[12] E.J. MITTEMEIJER, Journal of Metals (1985) p.16-20

[13] E.J. MITTEMEIJER, M.A.J. SOMERS, Proc. Int. Conf. on High Nitrogen Steels, Lille, France (1989)

[14] R.E. SCHACHERL, P.C.J. GRAAT, E.J. MITTEMEIJER, Metallurgical and Materials Transactions A 35 (2004) p. 3387-98

[15] M.SENNOUR, P.H. JOUNEAU, C. ESNOUF, Journal of Materials Science 39 (2004) p.1-11

[16] B. MORTIMER, P. GRIEVESON, K.H. JACK, Scandinavian Journal of Metallurgy 1, (1972) p. 203-209

[17] P.C. VAN WIGGEN, H.C.F. ROZENDAAL, E.J. MITTEMEIJER, Journal of Materials Science (1985) p. 4562-4582

[18] M.A.J. SOMERS, R.M. LANKREIJER, E.J. MITTEMEIJER, Philosophical Magazine A 59 (1989) p. 353-378

[19] R.E. SCHACHERL, P.C.J. GRAAT, E.J. MITTEMEIJER, Z.Metallkunde 93 (2002) 5 p.468-477

[20] E.J. MITTEMEIJER, M.A.J. SOMERS, Surface Engineering 13 (1997) 6

A B S T R A C T

UN NUOVO APPROCCIO AI MECCANISMI DI INDURIMENTO NELLO STRATO DI DIFFUSIONE DEGLI ACCIAI LEGATI, CON STRUTTURA α NITRURATI IN FASE GASSOSA EFFETTI DI CROMO E ALLUMINIO: STUDIO SPERIMENTALE E DI SIMULAZIONE

Parole chiave: trattamenti termici, nitrurazione, acciaio, metallurgia fisica, caratterizzazione materiali

Sono stati studiati i meccanismi di indurimento nello strato di diffusione di ferro e acciai con struttura α nitrurati in fase gassosa, attraverso l'analisi degli effetti della presenza di cromo (leghe binarie ed acciai industriali) e di alluminio (acciaio industriale). Dopo la nitrurazione (520°C 48h), il bilancio di massa dell'azoto fra la concentrazione di azoto totale nella zona di diffusione, determinata sperimentalmente, e la concentrazione di azoto prevedibile in via teorica, rivela per ogni lega "un eccesso di azoto". Jack e Mittemeijer [1-3] hanno suggerito che le differenze in volume fra i nitruri semi-coerenti e la matrice induca la distorsione locale del reticolo della matrice, e ciò porti ad un aumento locale della solubilità dell'azoto nella matrice. Nel presente studio si propone un nuovo approccio, basato su calcoli termodinamici (software Thermo-Calc), confermati mediante diversi metodi di caratterizzazione (HRTEM, EDX e raggi X).

In effetti non si riscontra alcuna significativo "eccesso di N" in soluzione solida, ma la concentrazione totale nell'azoto si spiega con la precipitazione di nitruri complessi metallo-azoto (MN), isomorfi di CrN cubico a facce centrate, contenenti cromo, ferro (fino a 30 % atomico, a 50μm dalla superficie), molibdeno e vanadio. Durante il trattamento (520°C 48h), la frazione atomica di ferro nei nitruri complessi (MN) diminuisce e la corrispondente frazione atomica di azoto si diffonde all'interno.

L'aggiunta di alluminio nell'acciaio industriale permette di aumentare decisamente la concentrazione di azoto e l'indurimento ($\Delta=HV_x-HV_{iniziale}$). L'alluminio induce, nello strato di diffusione, precipitazione di Fe_4N e di $Fe_{2-3}N$ e di precipitati nei nitruri complessi metallo-azoto (MN) a struttura FCC, contenenti cromo, ferro e molibdeno.